J Mater Sci: Mater Electron

The investigation of the effect of K doping on the structural, magnetic, and magnetocaloric properties of $La_{1.4-x}K_xCa_{1.6}Mn_2O_7$ ($0.0 \le x \le 0.4$) double perovskite manganite

Arıçtan Tulga Coşkun[1], Selda Kılıç Çetin[2,*], and Ahmet Ekicibil[2]

[1] Department of Physics, Faculty of Sciences, Muğla Sıtkı Koçman University, Muğla, Turkey
[2] Department of Physics, Faculty of Sciences and Letters, Çukurova University, 01330 Adana, Turkey

Received: 22 November 2021
Accepted: 12 March 2022

ABSTRACT

In this study, the effect of potassium doping on the morphological, crystallographic, magnetic and magnetocaloric properties of $La_{1.4}Ca_{1.6}Mn_2O_7$ double perovskite produced by the sol–gel wet chemical method was investigated. XRD analysis reveals that all samples have different percentages of tetragonal I4/mmm space group (double perovskite) and orthorhombic Pnma (perovskite) space group with. All samples showed a ferromagnetic to paramagnetic transition and a systematic decrease in T_C values was observed from 250 K for $x = 0.0$ to 150 K for $x = 0.4$ sample due to the increased amount of K^+ due to the coexistence of different ferromagnetic and antiferromagnetic interaction ratios in the samples. A decrease in the magnetic entropy change values was also observed with the decrease in the ferromagnetic double exchange interaction, due to the fact that the Mn^{4+} ions increasing with the K^+ doping support the antiferromagnetic Mn^{4+}–O^{2-}–Mn^{4+} super-exchange interactions. For the field change of 1 T, the maximum magnetic entropy change for the sample $La_{1.4}Ca_{1.6}Mn_2O_7$ was found to be 1.0 Jkg^{-1} K^{-1} it decreased down to 0.68, 0.75 and 0.60 Jkg^{-1} K^{-1} for $La_{1.3}K_{0.1}Ca_{1.6}Mn_2O_7$, $La_{1.2}K_{0.2}Ca_{1.6}Mn_2O_7$, $La_{1.0}K_{0.4}Ca_{1.6}Mn_2O_7$, respectively. Experimental results indicate that the samples can be potential candidates for sub-room temperature magnetic cooling application.

1 Introduction

Cooling systems, which we are encounter in all areas of dail life, are widely used to keep our foods cool and living spaces at comfortable temperatures. The basis of all cooling processes carried out today is based on vapor-compression technology. Among the various alternative technologies that can be used in cooling applications, researchers focus on magnetic cooling technology. Magnetic cooling technology,

Address correspondence to E-mail: kilics@cu.edu.tr

https://doi.org/10.1007/s10854-022-08078-z
Published online: 24 March 2022

despite some practical difficulties, can be an alternative to the vapor-compression technology commonly used in daily life. Although the cooling systems used today are of low efficiency, they are mass-produced and sold all over the world due to their commercial value. On the other hand, magnetic cooling systems used for technological and scientific purposes at temperatures below room temperature have high efficiency. However, it is the cooling that can be applied around room temperature that is commercially important. Materials exhibiting sufficiently high magnetocaloric effect (MCE) to be used in magnetic cooling technology around room temperature have been achieved. It is now believed by the scientific community that magnetic cooling technology can be an alternative to the vapor-compression technology that has been widely used due to the development of such materials. Based on the above motivation, magnetic measurements of many compounds have been extensively made, with the consideration that the rare-earth elements and their alloys show large MCE. The year 1997 marked a turning point due to the finding of $Gd_5Si_2Ge_2$ alloy and its practical use in pilot applications in magnetic refrigerating [1, 2]. Nevertheless, since Gd and Gd-based alloys are very expensive, difficult to form and require large magnetic field changes to show high MCE, commercial- use of refrigerators made of these materials does not yet seem economical.

In the past years, manganite compounds with the chemical form $La_{1-x}A_xMnO_3$ (A can be a monovalent or a divalent ion) and display high MCE values around room temperature have been found [3–5]. It is a thought that manganite compounds have considerable potential for the improvement of magnetic cooling systems in commercial means because the negations seen in Gd and Gd-based alloys do not exhibit in these compounds. It is well known from the literature that physical properties such as Curie temperature (T_C), magnetic entropy change (ΔS_M), adiabatic temperature change (ΔT_{ad}) can be adjusted in a wide range depending on the oxidation state, ionic radius and doping concentration of the additive [6, 7]. There are many studies investigating the effects of monovalent ion, divalent ion and simultaneous doping of both ions on the structural, electrical and magnetic properties [8–10]. In these studies, it has been found that some magnetic and magnetocaloric properties are affected positively, some are negatively in a sample produced by monovalent or divalent ion doping. Except for $La_{1-x}A_xMnO_3$ manganite family, another family in the chemical form $A_{2-2x}B_{1+2x}Mn_2O_7$, the so-called double perovskite manganites (A is a trivalent rare-earth cation like La, Nd, or Pr and B is a divalent alkaline earth cation like Sr, Ca, or Ba) have also been extensively studied [11–16]. This double perovskite manganite family differs from common $La_{1-x}A_xMnO_3$ type perovskite manganite compounds with its layered crystal structures and anisotropic exchange-interactions [17]. The crystal structures of these compounds consist of MnO_2 bilayers stacked along the *c*-axis, separated by insulating (R, A)–O layers. Since these compounds contain layered structures, physical properties are affected even by small changes that may occur in their composition and crystal structures due to different elemental additives. The fact that the Curie transition temperatures of the compounds can be easily adjusted depending on the change in doping amounts and high ΔS_M values are obtained at very low magnetic field changes, make these compounds high candidate materials for use in magnetic cooling applications. In this article, the structural, morphological, magnetic and magnetocaloric effect properties of $La_{1.4-x}K_xCa_{1.6}Mn_2O_7$ (x = 0.0, 0.1, 0.2, and 0.4) double perovskite manganite were investigated.

2 Experimental procedure

2.1 Sample synthesis

$La_{1.4}Ca_{1.6}Mn_2O_7$, $La_{1.3}K_{0.1}Ca_{1.6}Mn_2O_7$, $La_{1.2}K_{0.2}Ca_{1.6}Mn_2O_7$, $La_{1.0}K_{0.4}Ca_{1.6}Mn_2O_7$ double perovskite manganites were prepared by sol–gel method. The details of the sol–gel preparation procedure can be found elsewhere [18]. For convenience throughout the study, the compounds $La_{1.4}Ca_{1.6}Mn_2O_7$, $La_{1.3}K_{0.1}Ca_{1.6}Mn_2O_7$, $La_{1.2}K_{0.2}Ca_{1.6}Mn_2O_7$, $La_{1.0}K_{0.4}Ca_{1.6}Mn_2O_7$ are labeled as LCM1, LCM2, LCM3 and LCM4, respectively. After the powder samples obtained from the sol–gel process were ground, they were pressed into pellets under 3 tons. Then pressed samples were sintered at 1000 °C for 24 h in an air atmosphere and cooled down to room temperature in the furnace.

2.2 Characterization methods

The morphologies of the samples were investigated by field emission scanning electron microscope (FESEM, JEOL, JSM 5800). The crystallographic properties of the samples (crystal symmetry, phase purity, unit cell parameters and volumes) were characterized using the Bruker D2 Phaser X-ray Diffractometer with CuK_α (λ = 1.54056 Å) radiation at room temperature from 20° to 100° at a 2θ step of 0.01°. The temperature and field dependencies of magnetization [$M(T)$ and $M(H)$] were collected using a Quantum Design-Physical Properties Measurement System (PPMS). $M(T)$ was measured under 25 mT in zero-field-cooled (ZFC) and field-cooled (FC) sequences. In the ZFC sequence, the sample is first cooled down to 5 K under zero-field. Then, a field of 25 mT was applied, and the magnetization was measured up to 320 K. Subsequently, without removing the field, the magnetization was measured in the FC sequence down to 5 K. In order to determine the magnetocaloric properties, $M(H)$ isotherms were taken with increasing and decreasing fields between 0 and 5 T at constant temperatures around T_C in 4 K increments.

The magnetic entropy changes (ΔS_M) are calculated using $M(H)$ curves, by means of the thermodynamical equations of Maxwell which relates the magnetic entropy change with magnetization:

$$\Delta S_M(T,H) = \int_0^H \left(\frac{\partial M}{\partial T}\right)_H \mathrm{d}H \tag{1}$$

For practical reasons, the above integral is approximated with a summation and the derivative in the integral with the finite difference form, with discrete magnetization values at discrete temperatures and applied fields, as follows;

$$(\Delta S_M)_i = \sum_j \frac{M(T_{i+1},H_j) - M(T_i,H_j)}{T_{i+1} - T_i}(H_{j+1} - H_j) \tag{2}$$

where $(\Delta S_M)_i$ is the magnetic entropy change at a temperature T_i, M_i and M_{i+1} are the experimental values of the magnetizations obtained at the temperatures T_i and T_{i+1} under the magnetic field H_j.

3 Results and discussion

3.1 X-ray diffraction (XRD) pattern analysis

Figure 1 shows the typical XRD patterns of polycrystalline $La_{1.4-x}K_xCa_{1.6}Mn_2O_7$ (x = 0.0, 0.1, 0.2, and 0.4) compounds. All lines in the patterns have been indexed together according to the probability of the tetragonal I4/mmm space group (double perovskite) and the orthorhombic Pnma (perovskite) space group. The lattice parameters obtained for the samples are compatible with those obtained in the studies conducted in the literature [18, 19]. The structural parameters volume fraction for the parent and the K^+-doped compounds were obtained by refining the experimental data using the MAUD program and are listed in Table 1. It is found that the lattice parameters were decreased nearly unsystematically with increasing K^+ concentration. With the addition of K^+ ions into the crystal structure, the volume fraction of the tetragonal structure decreased. However, despite the increasing amount of K^+ ions in the crystal structure, the volume fraction of tetragonal and orthorhombic crystal structures in the doped compounds remained almost the same.

3.2 Scanning electron microscopy (SEM) analysis

The scanning electron microscopy (SEM) was used to examine the microstructure, grain diameter and grain size distribution of the compounds. The SEM micrographs of the samples are given in Fig. 2. The average grain sizes of the samples were calculated using Image J software and the average grain size histograms of the samples are given in Fig. 3. It is seen that increasing K^+ concentration level has made almost no considerable changes in grain size for the samples, with the exception of LCM3. It is observed from the SEM photographs and histograms; the average grain size of these samples varies between 400 and 440 nm and these compounds have homogeneous grain formation and uniform grain distribution. But the average grain size of the LCM3 sample is about 284 nm, which is smaller than the others. Considering that the ion radius of K^+ is larger than that of Ca, the decrease in grain size of the LCM3 sample due to the increased amount of K^+ is not an expected result. The SEM image of LCM1 manganite shows that the grains are not tightly

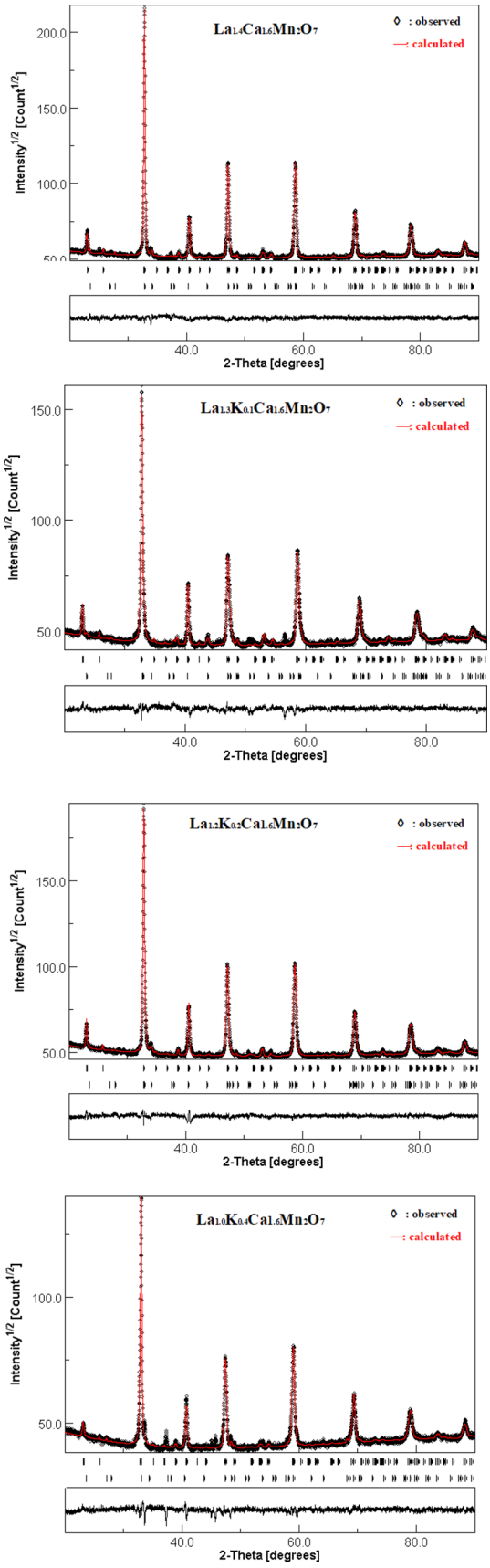

◀**Fig. 1** Observed and calculated XRD data and refinement for $La_{1.4-x}K_xCa_{1.6}Mn_2O_7$ (x = 0.0, 0.1, 0.2, and 0.4) samples

bound, contain porous structure, irregular spherical-like and polygonally formed in random directions. The grain formation of undoped LCM1 is like a combination of several small grains that gather as groups in the structure. However, it is seen that the grains become more spherical and homogeneous depending on the increasing K^+ concentration. As a result of K^+ addition, porous structure gradually disappeared, resulting in tightly bound grains and a morphology with less porosity. All compounds were pressed under the same pressure and subjected to the same heat treatment steps. The only difference in these stages is the number of larger radius K^+ ions that replace the Ca ions in the compounds. Therefore, during the crystallization stage depending on the heat treatment, there is a competition between the possibilities of either combining grains with another, remaining as an isolated grain, or combining with existing particles while the grain formation. Depending on the result of this competition, changes in surface morphology may occur on the surface of the samples. Therefore, it is expected that the morphology of the samples will affect the magnetic properties [20].

3.3 Magnetic properties

The temperature dependence of magnetization was measured using zero-field cooling (ZFC) and field-cooling (FC) processes. Figure 4 shows the $M-T$ curves of the samples under ZFC and FC conditions for an applied field of 25 mT. All samples showed a ferromagnetic to paramagnetic transition, called Curie temperature (T_C) and their values were found to be 250, 200, 175, and 150 K for the LCM1, LCM2, LCM3 and LCM4, respectively. It can be seen from Fig. 4 that replacing La^{3+} by K^+ causes the value of T_C to shift towards to low-temperature region. It can be said that the K^+-doped samples show a weak ferromagnetic behavior at temperatures above T_C due to the short-range FM spin interactions observed in the double-layered manganites [21]. Since the amount of calcium in the compounds is the same for all samples, the number of Mn^{4+} ions in the crystal structure is the same due to the presence of Ca ions in the compounds. However, for the K^+- doped

Table 1 The structural parameters obtained by refining with the MAUD program for the samples

$La_{1.4}Ca_{1.6}Mn_2O_7$		$La_{1.3}K_{0.1}Ca_{1.6}Mn_2O_7$		$La_{1.2}K_{0.2}Ca_{1.6}Mn_2O_7$		$La_{1.0}K_{0.4}Ca_{1.6}Mn_2O_7$	
Tetragonal (I4/mmm)	Orthorhombic (Pnma)	Tetragonal (I4/mmm)	Orthorhombic (Pnma)	Tetragonal (I4/mmm)	Orthorhombic (Pnma)	Tetragonal (I4/mmm)	Orthorhombic (Pnma)
a: 3.8562 Å	*a*: 5.4513 Å	*a*: 3.8246 Å	*a*: 5.4480 Å	*a*: 3.8516 Å	*a*: 5.4474 Å	*a*: 3.8290 Å	*a*: 5.4184 Å
b: 3.8562 Å	*b*: 7.6951 Å	*b*: 3.8246 Å	*b*: 7.6880 Å	*b*: 3.8516 Å	*b*: 7.6884 Å	*b*: 3.8290 Å	*b*: 7.6388 Å
c: 19.2488 Å	*c*: 5.4663 Å	*c*: 19.2548 Å	*c*: 5.4684 Å	*c*: 19.1884 Å	*c*: 5.4627 Å	*c*: 19.1557 Å	*c*: 5.4429 Å
Volume fraction: % 47.1	Volume fraction: % 52.9	Volume fraction: % 24.6	Volume fraction: % 75.4	Volume fraction: % 21.6	Volume fraction: % 78.4	Volume fraction: % 21.5	Volume fraction: % 78.5

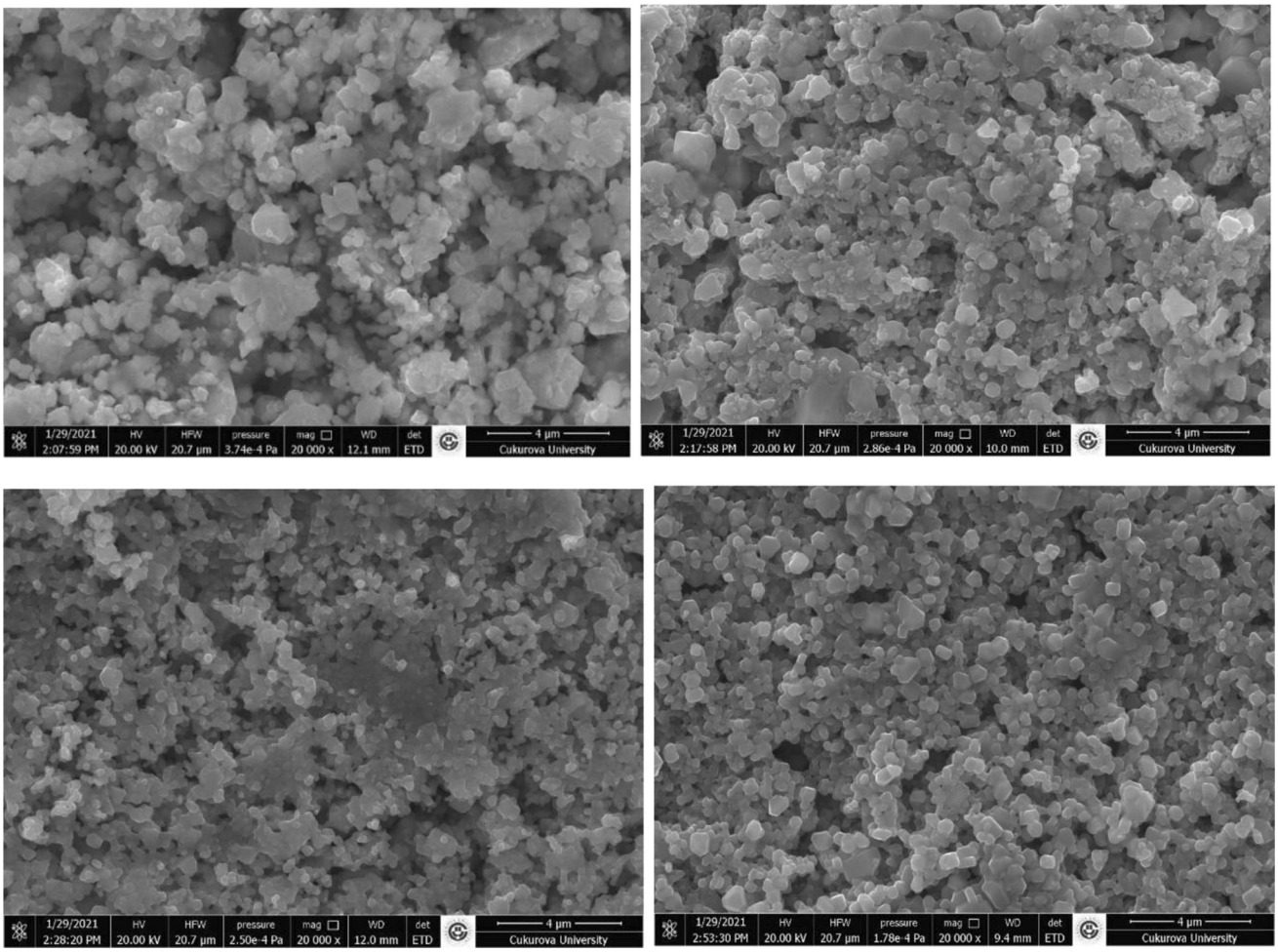

Fig. 2 Scanning electron micrograph of $La_{1.4-x}K_xCa_{1.6}Mn_2O_7$ for x = 0, 0.1, 0.2, and 0.4 samples

samples, we have to consider some chemical states. The replacement of some La ions with K^+ ions in the compounds will cause a gradual increase in the number of Mn $^{4+}$ atoms in the structure due to the amount of K^+ ions. It is well known that each K^+ ion oxidizes two Mn^{3+} ions to Mn^{4+} ions. Therefore, the occurrence of the antiferromagnetic Mn^{4+}–O^{2-}–Mn^{4+} super-exchange interactions will increase in compounds due to the increasing amount of K^+ ions. We can say that the systematic decrease in the *Tc* values

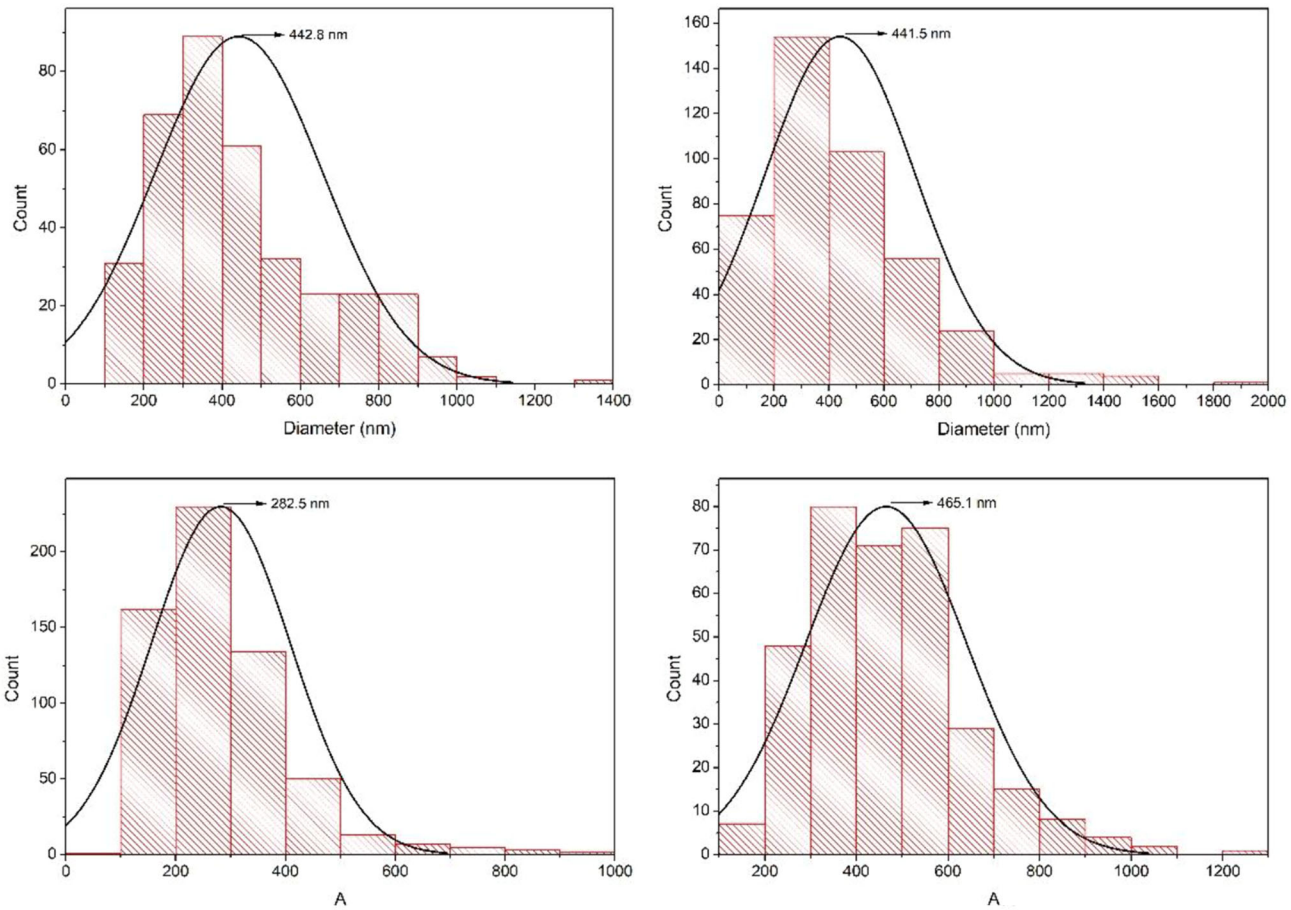

Fig. 3 The size distribution histogram of $La_{1.4-x}K_xCa_{1.6}Mn_2O_7$ for x = 0, 0.1, 0.2, and 0.4 samples

of the compounds due to the increasing amount of K^+ is due to the coexistence of different rates of ferromagnetic and antiferromagnetic interactions in the samples and the antiferromagnetic interactions becoming more dominant with the increase of Mn^{4+} ions in the structure. When the magnetization measurement is performed under the FC process, $M(T)$ curve in a PM-FM transition temperature range is expected to increase sharply straight with decreasing temperature up to the demagnetization limit and remain constant on the way to the low-temperature region [17]. For the studied compounds, the magnetic transition has occurred over a short temperature range (almost sharp transition) for LCM1 and this transition region widened with increasing K^+ concentration in the samples.

During the temperature-dependent magnetization measurements, the samples are either cooled in a zero magnetic field or cooled in a weakly applied magnetic field. During the experiment, the response of the magnetic spins to the applied magnetic field in the samples is due to both the strength of the applied magnetic field and the magnetocrystalline anisotropy energy [22, 23]. If the anisotropy field is large compared to the applied magnetic field, in this case, the applied external magnetic field will not be sufficient to align all the spins in the direction of the applied magnetic field [24]. Hence, the bifurcation between the FC and ZFC curves is strongly dependent on both the applied magnetic field and the magnetocrystalline anisotropy energy. Therefore, different net magnetizations are obtained due to the different spin orientation occurring in the field applied or untreated material [17]. Therefore, the degree of the bifurcation between the FC and ZFC curves is strongly dependent on both the applied magnetic field and the magnetocrystalline anisotropy energy. Similar deviations between ZFC–FC curves in low-temperature regions are observed in spin glasses and superparamagnetic nanoparticles [25]. In addition, a similar ZFC–FC magnetization curve was observed in phase-separated manganite compounds with co-existing

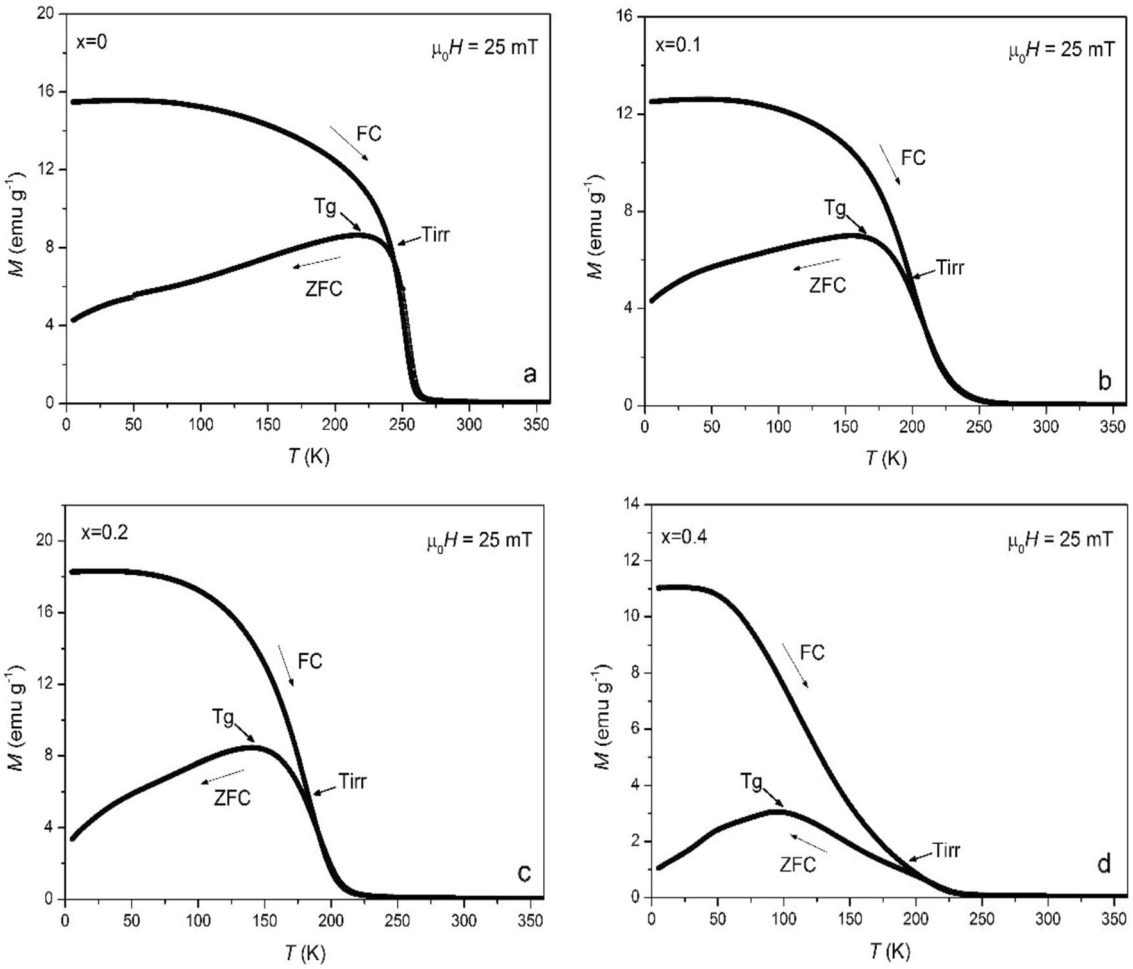

Fig. 4 The $M-T$ curves of the samples under ZFC and FC **a** $La_{1.4}Ca_{1.6}Mn_2O_7$, **b** $La_{1.3}K_{0.1}Ca_{1.6}Mn_2O_7$, **c** $La_{1.2}K_{0.2}Ca_{1.6}Mn_2O_7$, **d** $La_{1.0}K_{0.4}Ca_{1.6}Mn_2O_7$

ferromagnetic clusters and antiferromagnetic matrix [26].

Although the same external magnetic field is applied to all samples, a large bifurcation was observed between ZFC and FC curves towards lower temperatures depending on the increasing amount of K^+ concentration. Based on this result, we can say that the magnetocrystalline anisotropy in the compounds increases further with increasing K^+ amount. The separation between the ZFC–FC curve has started at a temperature, also called the irreversibility temperature (*Tirr*), and this separation became more evident towards lower temperatures for all samples. This obvious separation between ZFC–FC curves in K^+-doped samples is known as a typical magnetic property observed in spin-glasses systems [27]. A broad peak was seen in the ZFC curves of each sample after the bifurcation point. This peak is also called spin-glass freezing temperature (*Tg*), where the system goes to a glassy state below this temperature and is also considered a characteristic behavior of disordered systems [27]. When the amount of K^+ concentration in the samples was increased, the peak gradually expanded and shifted to lower temperatures.

The magnetic field dependence of magnetizations of the samples was measured at certain constant temperatures below and above *Tc* (in 4 K increments) at a magnetic field increase of 0.1 mT from 0 to 5 T and the results are shown in Fig. 5. At temperatures where the compounds show ferromagnetic properties, it is expected that the magnetization will increase rapidly with a low magnetic field due to the rapid growth of the ferromagnetic domains, and it will reach saturation with the increasing magnetic field. Although it was observed that the magnetizations

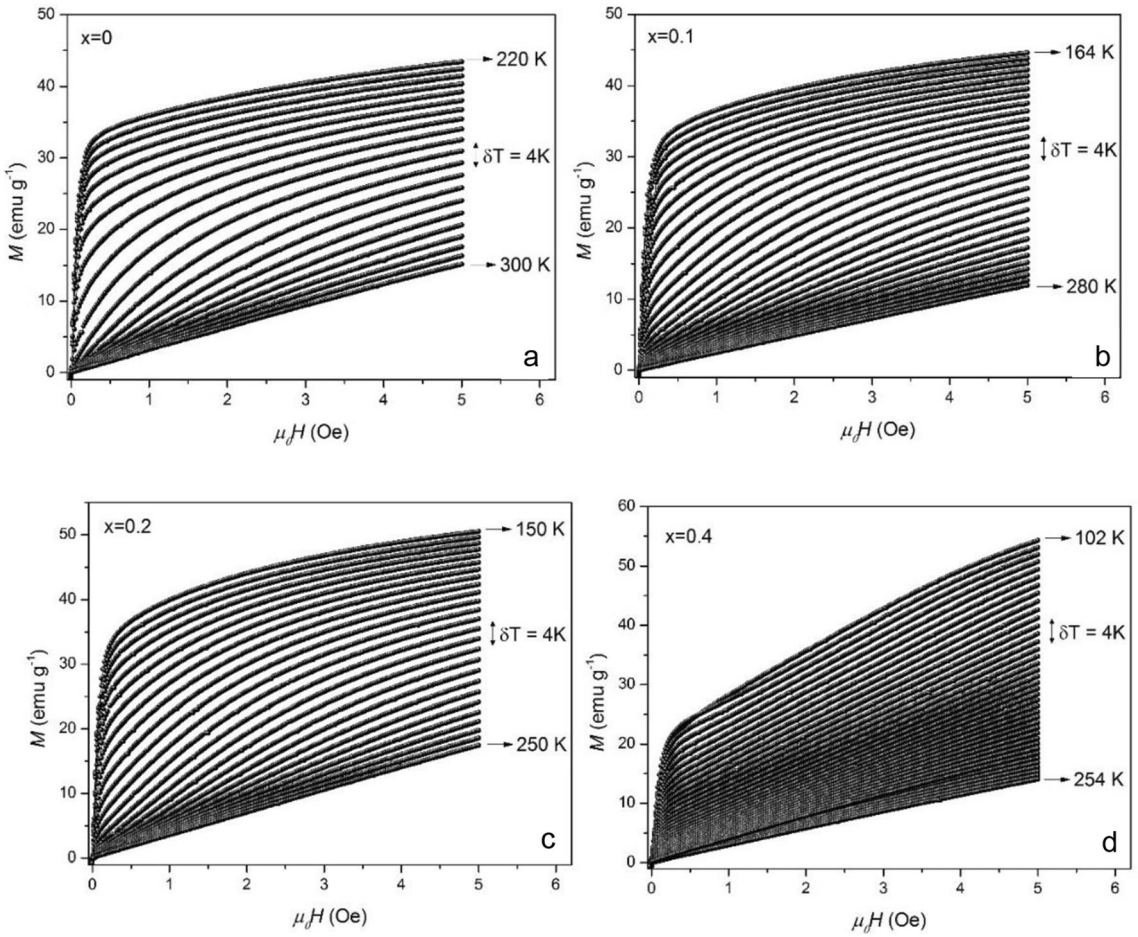

Fig. 5 Magnetization versus applied magnetic field $\mu_o H$ at different temperatures for the samples: **a** $La_{1.4}Ca_{1.6}Mn_2O_7$, **b** $La_{1.3}K_{0.1}Ca_{1.6}Mn_2O_7$, **c** $La_{1.2}K_{0.2}Ca_{1.6}Mn_2O_7$, **d** $La_{1.0}K_{0.4}Ca_{1.6}Mn_2O_7$

increased rapidly at low fields in all compounds in the ferromagnetic region, it was observed that none of the compounds reached saturation at high fields. It is seen that it is difficult to reach saturation in high magnetic fields, especially due to the increase in the K^+ concentration in the compounds. It can be said that the antiferromagnetic phase becomes more dominant due to the increase in the K^+ concentration in the compounds. Because it is known that the probability of Mn^{4+}–O^{2-}–Mn^{4+} antiferromagnetic super-exchange interactions will increase depending on the number of Mn^{4+} ions increasing as a result of increasing K^+ concentration. Above *Tc*, magnetization curves increased linearly with the applied magnetic field, which is indicative of typical paramagnetic behavior. A significant change in magnetization curves was seen around the T_C of the LCM1, indicating a remarkable magnetocaloric effect. However, it was observed that this change gradually decreased with increasing K^+ concentration.

In Fig. 6, the temperature dependence of the magnetic entropies ($|\Delta S_M|$) corresponding to five different field (1–5 T) changes is given. The maximum magnetic entropy changes under an applied magnetic field change of from 0 to 1 T were calculated as 1.0, 0.68, 0.75 and 0.60 $Jkg^{-1}\,K^{-1}$ for the LCM1, LCM2, LCM3, LCM4, respectively. The maximum magnetic entropy change of LCM1 appears to be higher than that of the K^+-doped samples.

As is well known, just because a compound has a high T_C value does not mean that the compound will have a high $|\Delta S_M|$. It is well known that the high magnetic entropy change in manganite compounds occurs from a rapid change of magnetization close to the transition temperature in the compound, from the sharpness of the $M-T$ curve during the ferromagnetic–paramagnetic phase transition, variation of the

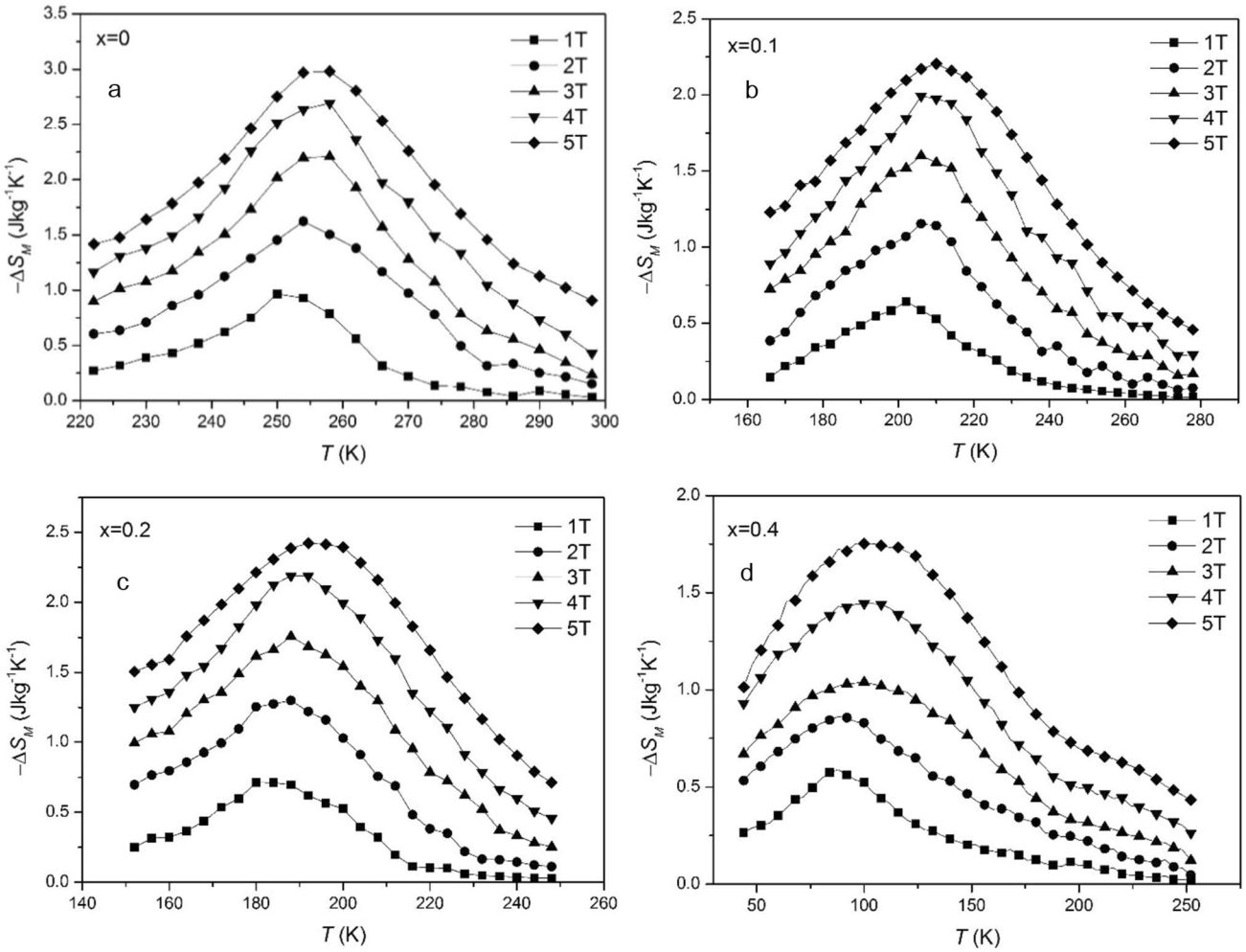

Fig. 6 The temperature dependence of $|\Delta S_M|$ for the samples: **a** $La_{1.4}Ca_{1.6}Mn_2O_7$, **b** $La_{1.3}K_{0.1}Ca_{1.6}Mn_2O_7$, **c** $La_{1.2}K_{0.2}Ca_{1.6}Mn_2O_7$, **d** $La_{1.0}K_{0.4}Ca_{1.6}Mn_2O_7$

ferromagnetic and antiferromagnetic interactions between Mn^{3+} and Mn^{4+} ions and strong spin–lattice interactions during the magnetic ordering process [28]. It is also necessary to take into account changes in Mn–O bond length, Mn–O–Mn bond angle, and lattice parameters that contribute to spin order or disorder. Among the potassium-doped samples, it is seen that the LCM3 sample has a higher maximum magnetic entropy value than the other two K^+-doped samples. The maximum magnetic entropy behavior of the LCM3 sample in the K^+-doped samples contradicts the T_C behavior of the K^+-doped samples. Although the T_C value of this sample was lower than that of the LCM2 sample, the $|\Delta S_M|$ values were found to be higher.

The maximum magnetic entropy change values increased with increasing magnetic field for all compounds. However, a shift was observed in the maximums of the magnetic entropy changes of the samples towards higher temperatures depending on the increase in the applied magnetic field up to 5 T. There are two types of interaction mechanisms that compete within the compound and affect the magnetic properties of perovskite manganite compounds: the Mn^{3+}–O^{2-}–Mn^{4+} double-exchange interactions which are ferromagnetically coupled and the coupling between Mn^{3+}–O^2–Mn^{3+}, Mn^{4+}–O^{2-}–Mn^{4+} which are antiferromagnetic super-exchange interactions. It is known that the large ZFC and FC splitting observed below T_C in the $M-T$ curve of the samples indicates a short-range ferromagnetic order as a result of the coexistence of both ferromagnetic and antiferromagnetic interactions. So, this shift can be explained by the enhancement of ferromagnetic

double-exchange interaction between Mn^{3+} and Mn^{4+} with the increase of the applied magnetic field [29].

4 Conclusion

In summary, the double-layered $La_{1.4-x}K_xCa_{1.6}Mn_2O_7$ (x = 0.0, 0.1, 0.2, and 0.4) manganites were synthesized by sol–gel method, where all samples have different volume percentages of tetragonal I4/mmm (double perovskite) and orthorhombic Pnma (perovskite) space groups. The structural and magnetic measurements were carried out systematically for all samples. The T_C decreased from 250 to 100 K as the K^+ content in lanthanum manganite increased from 0.1 to 0.4. It is possible to attribute these decreases to the increased number of Mn^{4+} ions as a result of the introduction of more K^+ ions into the crystal structure. This decrease in T_C can be explained in terms of an increase in Mn^{4+} content, decreasing the double-exchange interaction between Mn^{3+}–O^{2-}–Mn^{4+}, increasing the Mn^{4+}–O^{2-}–Mn^{4+}super-exchange interaction. Because the number of antiferromagnetic Mn^{4+}–O^{2-}–Mn^{4+} super-exchange interactions between increasing Mn^{4+} ions will increase. Thus, increasing antiferromagnetic interactions became dominant in the perovskite phase compared to ferromagnetic interactions, causing the T_C values to shift to lower temperatures. In addition, there are obvious differences between FC and ZFC magnetization curves at low temperatures, defining a spin-glass-like behavior. The splitting between FC and ZFC curves increased as the K^+ concentration increased in the samples. These have resulted from the frustration of randomly competing ferromagnetic double-exchange and antiferromagnetic super-exchange interactions, along with anisotropy arising from the layered structure. The maximum magnetic entropy changes of $La_{1.4}Ca_{1.6}Mn_2O_7$ were calculated to be higher than that of K^+-doped ones. The substitution of K for La decreased both T_C and maximum magnetic entropy change of the samples. Doping an x amount of K^+ introduces 2 × Mn^{4+} ions into Mn^{4+} ions in the compounds and antiferromagnetic Mn^{4+}–O^{2-}–Mn^{4+}super-exchange interactions increase, this process favors super-exchange interactions and consequently reduces ferromagnetic double-exchange interaction. In addition to these, the increase in the percentage of orthorhombic phase included in the structure with the addition of K^+ also shows that it causes a decrease in T_C and ΔS_M values. Besides, the magnetic entropy change results show that the studied samples can be considered to be a potential candidate for sub-room temperature magnetic cooling application.

Acknowledgements

The authors declare that no funds, grants, or other support were received during the preparation of this manuscript.

Author contributions

ATC & SKÇ performed the synthesis, structural and magnetic measurements of the samples under the guidance of AE. All authors contributed to the writing of the article.

Funding

The authors have not disclosed any funding.

Data availability

The datasets generated during and/or analyzed during the current study are available from the corresponding author on reasonable request.

Declarations

Conflict of interest The authors declare that they have no known competing financial interest or personal relationships that could have appeared to influence the work reported in this paper.

References

1. V.K. Pecharsky, K.A. Gschneidner Jr., Giant magnetocaloric effect in $Gd_5(Si_2Ge_2)$. Phys. Rev. Lett. **78**, 4494 (1997)
2. V.K. Pecharsky, K.A. Gschneidner Jr., Phase relationships and crystallography in the pseudobinary system Gd_5Si_4–Gd_5Ge_4. J. Alloys Compd. **260**, 98 (1997)
3. Z.B. Guo, Y.W. Du, J.S. Zhu, H. Huang, W.P. Ding, D. Feng, Large magnetic entropy change in perovskite-type manganese oxides. Phys. Rev. Lett. **78**, 1142 (1997)

4. B.F. Yu, Q. Gao, B. Zhang, X.Z. Meng, Z. Chen, Review on research of room temperature magnetic refrigeration. Int. J. Refrig. **26**, 622–636 (2003)
5. W. Zhong, W. Chen, W. Ding, N. Zhang, Y. Du, Q. Yan, Magnetocaloric properties of Na-substituted perovskite-type manganese oxides. Solid State Commun. **106**, 55–58 (1998)
6. M.H. Phan, S.B. Tian, D.Q. Hoang, S.C. Yu, C. Nguyen, A.N. Ulyanov, Large magnetic-entropy Change Above 300K in CMR materials. J. Magn. Magn. Mater. **25–259**, 309–311 (2003)
7. J. Fan, L. Pi, L. Zhang, W. Tong, L. Ling, B. Hong, Y. Shi, W. Zhang, D. Lu, Y. Zhang, Magnetic and magnetocaloric properties of perovskite manganite $Pr_{0.55}Sr_{0.45}MnO_3$. Physica B **406**, 2289–2292 (2011)
8. N. Abdelmoula, E. Dhahri, N. Fourati, L. Reversat, Monovalent effects on structural, magnetic and magnetoresistance properties in doped manganite oxides. J. Alloys Compd. **365**, 25–30 (2004)
9. N. Abdelmoula, A. Cheikh-Rouhou, L. Reversat, Structural, magnetic and magnetoresistive properties of $La_{0.7}Sr_{0.3-x}Na_{x}MnO_3$ manganites. J. Phys. Condens. Matter. **13**, 449–458 (2001)
10. L.E. Hueso, P. Sande, D.R. Miguéns, J. Rivas, Tuning of the magnetocaloric effect in $La_{0.67}Ca_{0.33}MnO_{3-\delta}$ nanoparticles synthesized by sol–gel techniques. J. Appl. Phys. **91**, 9943–9947 (2002)
11. T.G. Perring, G. Aeppli, Y. Moritomo, Y. Tokura, Antiferromagnetic short range order in a two-dimensional manganite exhibiting giant magnetoresistance. Phys. Rev. Lett. **78**, 3197 (1997)
12. H. Asano, J. Hayakawa, M.T. Matsui, Two-dimensional ferromagnetic ordering and magnetoresistance in the layered perovskite $La_{2-2x}Ca_{1+2x}Mn_2O_7$. Phys Rev B **56**(9), 5395–5403 (1997)
13. Y. Moritomo, Y. Maruyama, T. Akimoto, A. Nakamura, Metal-insulator transition in layered manganites: $(La_{1-z-}Nd_z)_{1.2}Sr_{1.8}Mn_2O_7$. Phys. Rev. B **56**, R7057 (1997)
14. C.D. Ling, J.E. Millburn, J.F. Mitchell, D.N. Argyriou, J. Linton, H.N. Bordallo, Bordallo, Interplay of spin and orbital ordering in the layered colossal magnetoresistance manganite $La_{2-2x}Sr_{1+2x}Mn_2O_7$ ($0.5<\sim x<\sim 1.0$). Phys. Rev. B **62**, 15096 (2000)
15. A.I. Coldea, S.J. Blundell, C.A. Steer, J.F. Mitchell, F.L. Pratt, Spin freezing and magnetic ınhomogeneities in bilayer manganites. Phys. Rev. Lett. **89**, 277601 (2002)
16. G. Allodi, M. Bimbi, R. De Renzi, C. Baumann, M. Apostu, R. Suryanarayanan, A. Revcolevschi, Magnetic order in the double-layer manganites $(La_{1-z}Pr_z)_{1.2}Sr_{1.8}Mn_2O_7$: intrinsic properties and role of intergrowth. Phys. Rev. B **78**, 064420 (2008)
17. E. Tasarkuyu, A. Coskun, A.E. Irmak, S. Aktürk, G. Ünlü, Y. Samancıoglu, A. Yücel, C. Sarıkürkcü, S. Aksoy, M. Acet, Effect of high temperature sintering on the structural and the magnetic properties of $La_{1.4}Ca_{1.6}Mn_2O_7$. J. Alloys Compd. **509**, 3717–3722 (2011)
18. A.E. Irmak, E. Taşarkuyu, A. Coşkun, S. Aktürk, Z. Dikmen, Ö. Orhun, Structural electrical and magnetic properties of high temperature sintered $La_{1-x}Na_xMnO_3$ ($0.05 \leq x \leq 0.35$) compounds. J. Electron. Mater. **44**, 326–331 (2015)
19. S.J. Hibble, S.P. Cooper, I.D. Fawcett, A.C. Hannon, M. Greenblatt, Local distortions in the colossal magnetoresistive manganates $La_{0.70}Ca_{0.30}MnO_3$, $La_{0.80}Ca_{0.20}MnO_3$ and $La_{0.70}Sr_{0.30}MnO_3$ revealed by total neutron diffraction. J. Phys.: Condens. Matter. **11**, 9221–9238 (1999)
20. S.K. Çetin, G. Akça, M.S. Aslan, A. Ekicibil, Role of nickel doping on magnetocaloric properties of $La_{0.7}Sr_{0.3}Mn_{1-x}Ni_{x-}O_3$ manganites. J. Mater. Sci.: Mater. Electron. **32**, 10458–10472 (2021)
21. H. Asano, J. Hayakawa, M. Matsui, Two-dimensional ferromagnetic ordering and magnetoresistance in the layered perovskite $La_{2-2x}Ca_{1+2x}Mn_2O_7$. Phys. Rev. B **56**, 5395 (1997)
22. R. Revathy, M.R. Varma, K.P. Surendran, Effect of morphology and ageing on the magnetic properties of nickel nanowires. Mater. Res. Bull. **120**, 110576 (2019)
23. P.A. Joy, P.S.A. Kumar, S.K. Date, The relationship between field-cooled and zero-field-cooled susceptibilities of some ordered magnetic systems. J. Phys. Condens. Matter. **10**, 11049 (1998)
24. P.S.A. Kumar, P.A. Joy, S.K. Date, Comparison of the irreversible thermomagnetic behaviour of some ferro- and ferrimagnetic systems. Bull. Mater. Sci. **23**, 97–101 (2000)
25. R. Selmi, W. Cherif, L. Fernández Barquín, M. de la Fuente Rodríguez, L. Ktari, Structure and spin glass behavior in $La_{0.77}Mg_{0.23-x}MnO_3$ ($0 \leq x \leq 0.2$) manganites. J. Alloys Compd. **738**, 528–539 (2018)
26. I.G. Deac, J.F. Mitchell, P. Schiffer, Phase separation and low-field bulk magnetic properties of $Pr_{0.7}Ca_{0.3}MnO_3$. Phys. Rev. B **63**, 172408 (2001)
27. E. Fertman, S. Dolya, V. Desnenko, A. Beznosov, M. Kajnaková, A. Feher, Cluster glass magnetism in the phase separated $Nd_{2/3}Ca_{1/3}MnO_3$ perovskite. J. Magn. Magn. Mater. **324**, 3213–3217 (2012)
28. Y. Samancıoglu, A. Coskun, Magnetic properties of A- and B-site cation doped $La_{0.65}Ca_{0.35}MnO_3$ manganites. J. Alloys Compd. **507**, 380–385 (2010)

29. A. Coşkun, E. Taşarkuyu, A.E. Irmak, M. Acet, Y. Samancıoğlu, S. Aktürk, Magnetic properties of $La_{0.65}Ca_{0.30}Pb_{0.05}Mn_{0.9}B_{0.1}O_3$ (B=Co, Ni, Cu and Zn). J. Alloys Compd. **622**, 796–804 (2015)